the solution with dichloroethyl ether and discarded. A treatment with NaOH-Na_2O_2 precipitates nickel, cobalt, and manganese, and extracts the chromium in the form of chromate, which is precipitated with barium. The manganese is left in the form of MnO_2, and an extraction with concentrated HNO_3 separates it from nickel and cobalt. The MnO_2 is dissolved in HCl, reprecipitated with Na_2O_2, extracted with HNO_3, filtered and dried at 110°C. Nickel is precipitated with dimenthylglyoxime and then cobalt is precipitated with α-nitroso β-naphthol reagent.

(2) *Chromium, Manganese, Cobalt, Nickel, Copper, Zinc, and Gallium from Gallium*

Acid-soluable gallium oxide prepared by the decomposition of the nitrate at 250°C is used as the target. The target is dissolved in concentrated HNO_3 and carriers are added. Then the nitrates are converted to chlorides by fuming with HCl. Gallium is extracted with dicholoroethyl ether from 6*N* HCl solution and back extracted into water; an aliquot is precipitated with 8-hydroxyquinoline ("oxine") for counting.

Copper is reduced to metal with granulated tin. Zinc and chromium are separated by treatment with Na_2O_2. The chromium as chromate is precipitated with barium, and the zinc is precipitated with mercuric thiocyanate reagent. Manganese, cobalt, and nickel are separated as in Part (1).

(3) *Manganese, Cobalt, Nickel, Copper, Zinc, and Gallium from Germanium and Arsenic*

Germanium oxide or arsenious oxide are used as targets. The oxide is dissolved in a minimum of concentrated NaOH, after which the solution is made slightly acid with HCl. The carriers are added and precipitated with excess potassium ferrocyanide. An aliquot of the supernatant solution may be precipitated with H_2S to obtain germanium or arsenic activities.

The precipitated ferrocyanides are fumed with H_2SO_4 and the residue is dissolved in HCl. Copper is precipitated with granulated tin, which also reduces iron to the divalent state. Gallium is extracted with dichloroethyl ether, back extracted into water and precipitated with oxine.

Iron is then oxidized with H_2O_2, extracted with dichoroethyl ether and discarded. Zinc is separated by treatment with Na_2O_2, and precipitated for counting with mercuric thiocyanate. Manganese, cobalt, and nickel are separated as in Part (1).

PHYSICAL REVIEW VOLUME 97, NUMBER 5 MARCH 1, 1955

Yields of Photonuclear Reactions with 320-Mev X-Rays. II. Interpretation of Results*

I. HALPERN,† R. J. DEBS,‡ J. T. EISINGER,§ A. W. FAIRHALL,† AND H. G. RICHTER‖
Laboratory for Nuclear Science, Massachusetts Institute of Technology, Cambridge, Massachusetts

(Received September 20, 1954; revised manuscript received December 8, 1954)

It is convenient to separate the yields of radio-nuclides obtained in the work described in the preceding paper into two groups. The first group consists of the yields of nuclides which are only one or two mass units lighter than the target. All of the yields in this group, and especially those corresponding to (γ,n) reactions, are relatively large. They are due mainly to photons in the giant resonance region ($h\nu\sim 20$ Mev) of the x-ray spectrum, and account for most of the nuclear events produced in medium-weight targets by 320-Mev x-rays.

The yields of those radio-nuclides which are more than a few mass units lighter than the target are in many ways more interesting than the ones in the first group. They are found to exhibit a simple pattern very similar to those obtained in particle-induced high-energy reactions. It is shown that such patterns are at least qualitatively consistent with models of high-energy nuclear reactions in which the last few particles emitted from a struck nucleus, leave by "evaporation." Indeed the evaporation of these last particles exerts so strong an influence on the form of the observed yield pattern, that it becomes very difficult to say anything about either the nature of the original nuclear events or the emission of the first few particles on the basis of a study of yield patterns.

Finally, a rough quantitative comparison is made of the yields of radio-nuclides and the reported yields of neutrons and other particles emitted from medium-weight nuclei irradiated with 320-Mev x-rays.

IN the preceding paper, a number of relative yields are reported for the formation of radio-nuclides from the irradiation of medium weight elements by high-energy x-rays. In the following two sections, the yields for radio-nuclides which are more than a few mass units lighter than the target are shown to fall into simple patterns. These patterns are described quantitatively in Sec. 3 and it is shown that they are evidence for a major role of nuclear evaporation in high-energy photoreactions. It is found in Sec. 4 that the pattern described here is quantitatively very similar to patterns constructed from data of high-energy particle-induced reactions. An attempt is made in Sec. 5 to account for all of these patterns in a semiquantitative way by assuming that the last few particles ejected in a high-energy reaction are evaporated. Section 6 deals with those photoreaction yields in which the observed nuclide is only a few mass units lighter than the target. Finally, in Sec. 7, the data of this experiment are compared to data for neutron production and meson production by high-energy x-rays.

* This work was supported in part by the joint program of the Office of Naval Research and the U. S. Atomic Energy Commission.

† Now at the University of Washington.

‡ Now at Stanford University.

§ Now at Bell Telephone Laboratories.

‖ Now at the U. S. Naval Radiological Defense Laboratory, San Francisco, California.

1. YIELDS FROM ARSENIC

When the work described in the preceding paper was undertaken, only a few measurements had been made of the distribution of the residual nuclides in high-

energy nuclear reactions and none of these were for photoreactions. It was decided to observe photonuclear yields from a set of targets having consecutive atomic numbers in order to obtain a sufficient amount of data to establish any regularities of yield pattern.

Of the five elements used as targets, arsenic is the only one that is monoisotopic and its yields are therefore the easiest to interpret. The arsenic yields are plotted in Fig. 1 in a way designed to exhibit their regularity. It is seen that if the yields are expressed as a function of the atomic number and the atomic weight of the observed radio-nuclide, this function can be represented by a simple smooth surface. Lest it appear that the data of Fig. 1 seem rather meager for this conclusion, it should be mentioned that the data obtained from the other targets agree with the pattern for arsenic. Moreover, very similar surfaces have been reported for high-energy particle-induced reactions.[1,2]

Among the noteworthy features of the surface of Fig. 1 are the following: (1) The peak yields for any separated element occur near the stable valley of the nuclear energy surface (see Table I). (2) The yields of the various separated elements lie on very similar curves. (3) Corresponding points on these curves are separated by a constant factor of 2.3 in yield for each unit change in atomic number of the observed nuclide.

It should also be mentioned that the observed yields do not fit the pattern of Fig. 1 if the difference in atomic number between target and observed nuclide, ΔZ, is less than 2. These yields will be discussed separately (Sec. 6).

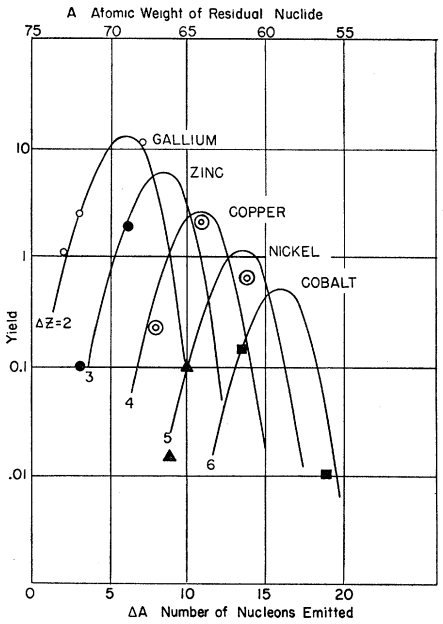

FIG. 1. The photonuclear yields from arsenic with 320-Mev x-rays, plotted as a function of ΔA, the number of nucleons emitted. Identical curves have been drawn through the data for each value of ΔZ, the change in nuclear charge in the reaction.

[1] E. Belmont and J. M. Miller, Phys. Rev. **95**, 1554 (1954).
[2] Rudstam, Stevenson, and Folger, Phys. Rev. **87**, 358 (1952).

TABLE I. The peaks of the yield surface in the photodisintegration of arsenic.

Separated element	Z	The atomic weight at the center of the stable valley[a]	The atomic weight at the peak of the yield surface
Gallium	31	69.4	69.0
Zinc	30	67.0	66.4
Copper	29	64.5	64.0
Nickel	28	61.4	61.3
Cobalt	27	58.9	58.8

[a] These numbers are based on characteristics of the nuclear energy surface described in reference 20.

2. YIELD SURFACES FOR THE TARGETS COPPER TO GERMANIUM

The comparison of yields from targets having more than one isotope to the yields from arsenic involves a certain amount of uncertainty. For multi-isotope targets each observed yield is a superposition of the yields from the various isotopes, and there is unfortunately no way of knowing how much each isotope contributes to the yield. In order to be able to see whether the yield patterns for such targets are consistent with the pattern for arsenic, it is necessary to assume some scheme for dividing up an observed yield among its possible parents.

The simplest such assumption, which will be called scheme 1, is that all target isotopes contribute to every yield in proportion to their abundance. Such an assumption would certainly not apply to yields which correspond to the emission of only one or two particles, but it might be reasonable for reactions in which $\Delta Z \geqslant 2$. In essence this assignment scheme assumes that the observed yield pattern is to a large measure independent of the exact mass of the target isotope.

The second procedure for dividing up yields, scheme 2, is also fairly easy to apply, but unlike scheme 1, it stresses the effect of the target mass on the observed distribution. In this scheme, one assumes that the relative probability of any two *reactions* is the same for all target isotopes.

Thus according to scheme 1, the yield of Co^{61}, for example, would be expected to be the same from a gram of Ga^{69} as from a gram of Ga^{71}. According to scheme 2, the yield of Co^{61} from Ga^{71} would be the same as the yield of Co^{59} from Ga^{69}.

In order to examine the consistency of the data under the assumption of scheme 1, the arsenic data of Fig. 1 were replotted to fall on a single curve in the following way. First each yield was multiplied by the factor $(2.3)^{\Delta Z}$. This brought all of the curves in Fig. 1, up to the same horizontal level. Then each modified yield point was replotted as a function of the "distance" of the corresponding radio-nuclide from the center of

the stable valley. By this distance we mean $(A-A_s)$, where A is the mass of a radio-nuclide and A_s is the mass at the center of the stable valley for the atomic number of the radio-nuclide. All of the arsenic data were made, in this way, to lie very nearly on the same simple curve. The next step was to treat the data for the other targets in exactly the same way. If it were now found that all of the data fell on a single curve, it would mean that all of the targets have an identical yield surface and the assumption underlying scheme 1 is correct. The data plotted in this way are shown in Fig. 2. This way of representing the data is very similar to the approach used by Belmont and Miller.[1]

In applying scheme 2, one begins again by replotting the arsenic data so that they lie on a single curve. The ordinate is once again the yield multiplied by $(2.3)^{\Delta Z}$ but the abscissa this time is related to ΔA, total number of nucleons emitted. In fact, it is $\Delta A-\Delta A_Z$ where ΔA_Z is the most probable number of nucleons emitted from arsenic when Z protons are lost. An example will show how data from targets other than arsenic are treated. Let Y represent the observed yield of Co^{61} in a copper bombardment. Some of Y is due to a $(\gamma,2p)$ reaction on Cu^{63} and some to $(\gamma,2p2n)$, possibly (γ,α), on Cu^{65}. According to the arsenic yield surface the second reaction is about eight times as probable as the first, but Cu^{63} is roughly twice as abundant as Cu^{65}. Hence $0.2Y$ is assigned to Cu^{63} and $0.8Y$ to Cu^{65}. These data can now be treated like the arsenic data and plotted on the same graph. (Fig. 3).

It is seen from Figs. 2 and 3 that either scheme, and especially scheme 1, serves to demonstrate a fairly consistent behavior of target nuclides in the copper-to-arsenic mass region. Scheme 1 does as well as one might expect considering only the experimental uncertainty in the data.

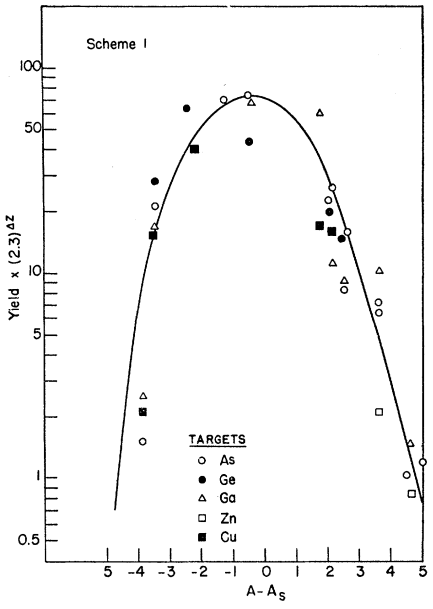

FIG. 2. Photonuclear yields with 320-Mev x-rays, plotted as a function of the distance (in units of atomic weight) of the observed nuclide from the center of the stable valley.

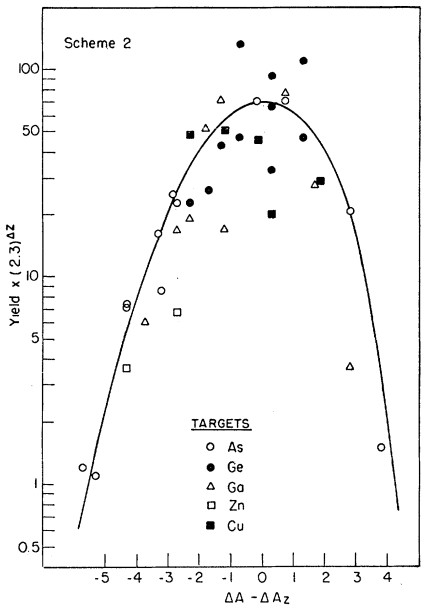

FIG. 3. Photonuclear yields with 320-Mev x-rays, plotted as a function of the number of nucleons emitted in the observed reaction. ΔA_Z is the most probable number of nucleons emitted for a given ΔZ according to the arsenic yield surface.

In a sense schemes 1 and 2 represent extreme assumptions about the nature of high-energy reactions. In general a given yield might be expected to depend on the nature of both the target and residual nuclides. According to scheme 1, there is practically no dependence on the target nuclide. Yields are determined by the location of the final nuclide with respect to the stable valley. According to scheme 2, any special properties of the residual nuclides have no bearing at all on the final distribution. The yield surface location depends only on the target nuclide location.

The fact that scheme 1 organizes the data somewhat more consistently than scheme 2 may indicate that the truth lies closer to the assumptions of scheme 1. That is, the shape of the yield surface depends more on the properties of the observed nuclides than on those near the starting point of the photoreaction. Such a conclusion is consistent with a strong role for evaporation processes in high-energy reactions. For according to an evaporation model, the probability of emitting a neutron or a proton from a given excited nucleus during a reaction does not depend on how many neutrons or protons have already been evaporated. The starting point of the reaction is easily forgotten. All that counts are the excitation energy and the binding energies of various particles to the intermediate nucleus. Since the relative neutron and proton binding energies are related to the position of the nuclide on the nuclear

energy surface, one might expect final yield patterns to be related to the nuclear energy surface.

In order to make more quantitative arguments for the role of nuclear evaporation in high-energy reactions, it is necessary to describe the photonuclear yield surfaces in somewhat more detail.

3. SHAPE OF THE YIELD SURFACE

The surface described in Figs. 1 and 2 is an inverted trough held at an angle to the plane of the isotope chart (see Fig. 4). It is possible to characterize this surface with three parameters: (1) The distance of the ridge from the stable valley. In the present experiment, the ridge stays fairly parallel to the valley at about half a mass unit to the neutron-deficient side. (2) The tilt of the ridge with respect to the N–Z plane. The ridge yield drops off by a factor of 2.3 for each unit change in Z. (3) The width of the trough. The width at half maximum seems to remain fairly constant and will be discussed in detail.

Although one might be tempted to interpret the closeness of the ridge to the stable valley as evidence for the role of evaporation in high-energy photoreactions, such an interpretation would not be entirely justifiable. If for any reason at all, proton emission happens to be on the average about $\frac{2}{3}$ as probable as neutron emission in this mass region, the peak yields would tend to occur near the stable valley.

It is the behavior of the third parameter, the yield surface width, that is the strongest evidence for the importance of nuclear evaporation in high-energy reactions. The particular value of the observed width as well as the fact that it stays nearly constant give evidence for the role of the nuclear energy surface in steering the particle emission process.

It is convenient to determine the numerical value of the width by passing a plane through the yield surface at constant A. The width at half maximum of the curves of intersection is found to be about 1.3 units of Z all along the surface. It is interesting to compare this to the result that one would expect for an uncorrelated sequence of nucleon emissions. Let us assume that only neutrons and protons can be emitted. (It can be shown that neglecting α particle emission does not seriously affect arguments about the surface width.) The expected width of the distribution resulting from the emission of $N+P=\Delta A$ nucleons, would be roughly $(\Delta A)^{\frac{1}{2}}$. That is, the width of the yield surface would increase noticeably as one leaves the neighborhood of the target. It would vary from about 2 to 4 for the range of ΔA covered in the present experiment. The observed width is definitely smaller than the widths estimated on this basis (see Fig. 5).

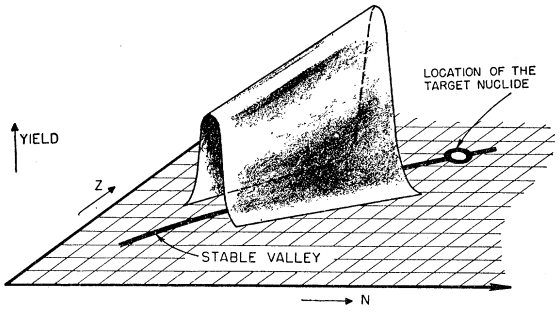

FIG. 4. A schematic representation of the portion of the photonuclear yield surface that has been examined in the present experiment.

It must be concluded that the emissions of successive particles are not uncorrelated. The sequence of emissions is channeled by some confining "forces" and the final distribution of nuclides is therefore considerably tighter than one could otherwise expect. It is reasonable to suspect that these "forces" are associated with the nuclear energy surface. Before looking into this suggestion quantitatively, it would be useful to compare the yield surfaces observed in so-called spallation or high-energy particle-induced reactions to the photoreaction surface of the preceding sections.

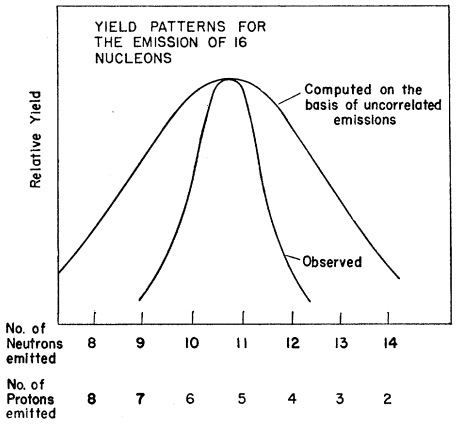

FIG. 5. A section taken through the yield surface at a constant atomic weight of the residual nucleus. The observed surface is much narrower than that to be expected on the basis of uncorrelated emission of nucleons.

4. YIELD SURFACES PRODUCED BY HIGH-ENERGY PARTICLE BOMBARDMENT

A considerable amount of information has been accumulated on the yields from nuclear reactions induced by high-energy particles. Bombardments have been made with high-energy protons,[1–5] neutrons,[6] deuterons,[3,7–9] and α particles.[3,9] Elements in a number of regions of the isotope chart have been investigated at

[3] Batzel, Miller, and Seaborg, Phys. Rev. **84**, 671 (1951).
[4] W. J. Worthington, Jr., University of California Radiation Laboratory Report 1627 (unpublished).
[5] W. E. Bennett, Phys. Rev. **94**, 997 (1954).
[6] L. Marquez, Phys. Rev. **88**, 225 (1952).
[7] M. Lindner and I. Perlman, Phys. Rev. **78**, 499 (1950).
[8] H. H. Hopkins, Jr., Phys. Rev. **77**, 717 (1950).
[9] Miller, Thompson, and Cunningham, Phys. Rev. **74**, 347 (1948).

energies up to 1.5 Bev.[10] Recently Templeton[11] has published a comprehensive review of this entire field. His interpretations of the role of nuclear evaporation in determining spallation patterns is similar to the one being developed here.

All of the yield surfaces observed in particle reactions have the general features of the photoreaction surface. Most of the data have been obtained for middle weight targets, and for such targets the yield surface widths are observed to be about 1.3 or 1.4 units of Z. The yield surface ridges for such targets lie roughly parallel to the stable valley at about a mass unit to the neutron deficient side. These features of the surfaces seem to be rather independent of the nature of the bombarding agent or its energy (provided that it is more than about 100 Mev). This independence is consistent with the notion that the shape of the yield surface depends mainly on the nature of the evaporation process (an aspect of the reactions that can easily be common to them all), rather than on any special features of the collisions initiating the reactions.

It has been somewhat more difficult to compare the remaining parameter, the slope of the ridge with respect to the N–Z plane, for the particle yield surfaces. This parameter is generally the one most poorly defined experimentally because the peak yields occur for nuclides near the center of the stable valley where most of the nuclides are stable and therefore unobservable. The widths and ridge locations can be determined fairly well nonetheless, because of the steepness of the sides of the yield surface. It is unfortunate that the ridge slope is so hard to determine, for it is the only parameter of the three that has to do with the nature of the original interaction. As Belmont and Miller[1] point out, it has to do with the distribution function for the energy made available in the nucleus by the original interaction. In some bombardments[1,2,12], it was possible to obtain yield data for radio-nuclides among the very light elements. These data indicate a leveling off of the ridge slope which is probably connected with the emission of α particles and other heavy fragments with relatively high probability.

5. EVAPORATION THEORY AND THE HIGH-ENERGY YIELD PATTERNS

A number of qualitative evidences have been discussed for the role of evaporation in high-energy nuclear reactions. It should be mentioned that there are experiments that show that not all the emitted particles are evaporated. The energy and angular distributions of particles observed in counter[13] and photographic plate[14–16] experiments seem to indicate that some particles are ejected from nuclei as a result of a succession of internal collisions started by an incoming fast particle. Bernardini[14] and others[17] have discussed such internal collision models in a fair amount of detail. Bernardini finds that after the collision part of the reaction is over, an average of 50 Mev of excitation energy is left behind in a nucleus of mass $A=100$. Presumably this energy is dissipated by the evaporation of some particles and some photons.

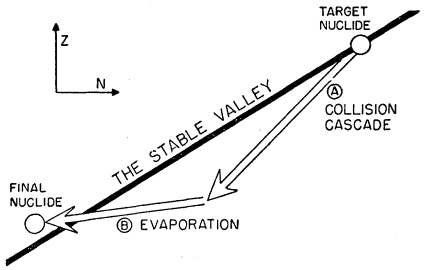

FIG. 6. A high-energy nuclear reaction can be imagined to take place in two steps. During the first step, particles are emitted more or less at random. During the second step they are evaporated.

We shall try to show that as long as enough energy remains on the average for the evaporation of four or five nucleons, the yield surfaces would be expected to have their observed features. The particle emission "trajectory" of a reaction, according to Bernardini's model, looks like the path A–B in Fig. 6. The starting point is a stable target nucleus and during the internal collision part of the reaction, along A, roughly equal numbers of neutrons and protons are emitted. It will be shown that during the final evaporation part of the reaction, B, the low average kinetic energy of emitted particles suppresses the emission of charged particles because of the Coulomb barrier. Mostly neutrons are emitted. The transition from A to B is probably less sharp than Fig. 6 would indicate.

The nature of the evaporation part of a high-energy reaction will be examined from the viewpoint of the statistical theory of Weisskopf.[18] A similar and more detailed treatment of this problem has been given by Le Couteur[19] in his explanation of prong distributions of cosmic ray stars. The main differences between the two treatments are that Le Couteur considers evaporations that start at rather higher energies than those involved here and that he is not specifically concerned with those implications of the evaporation process that have to do with the shapes of yield surfaces.

[10] Friedlander, Baker, Hudis, Miller, and Wolfgang, Phys. Rev. **94**, 775 (1954).
[11] D. H. Templeton, Ann. Rev. Nuc. Sci. **2**, 93 (1953).
[12] R. E. Batzel and G. T. Seaborg, Phys. Rev. **82**, 607 (1951); D. H. Greenberg and J. M. Miller, Phys. Rev. **84**, 845 (1951).
[13] J. Hadley and H. York, Phys. Rev. **80**, 345 (1950).
[14] Bernardini, Booth, and Lindenbaum, Phys. Rev. **85**, 826 (1952); **88**, 1017 (1952).
[15] Harding, Lattimore, and Perkins, Proc. Roy. Soc. (London) **A196**, 325 (1949).
[16] H. Fishman and A. M. Perry, Jr., Phys. Rev. **86**, 167 (1952).
[17] M. L. Goldberger, Phys. Rev. **74**, 1269 (1948); R. Serber, Phys. Rev. **72**, 1114 (1947).
[18] J. M. Blatt and V. F. Weisskopf, *Theoretical Nuclear Physics* (John Wiley and Sons, Inc., New York, 1952).
[19] K. J. Le Couteur, Proc. Phys. Soc. (London) **A63**, 259 (1950).

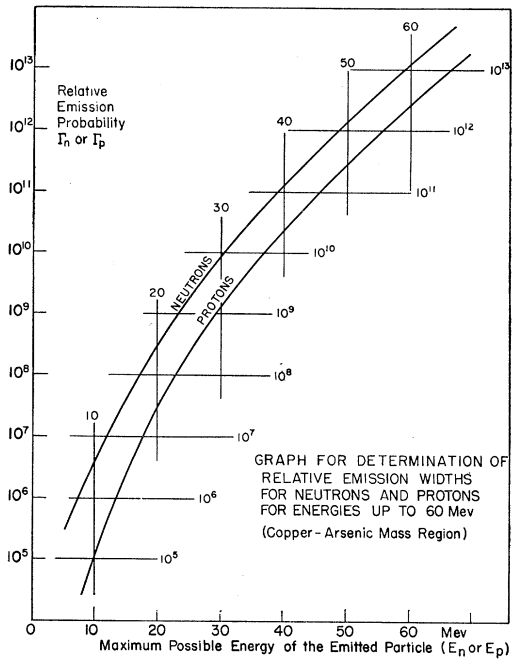

FIG. 7. These curves are based on the nuclear level densities given in Blatt and Weisskopf (see reference 18). They can be used to determine the ratio of protons to neutrons emitted from an excited nucleus if the excitation and binding energies are known.

It will be assumed to start with that only nucleons are evaporated from nuclei. Figure 7 shows a pair of curves from which relative probabilities for the evaporation of neutrons and protons can be determined for excited nuclei in the copper-arsenic region. These curves are essentially extensions of those given in Blatt and Weisskopf.[18] For a given excitation energy, one determines the ratio of ordinates for a pair of corresponding points, one on each curve. This number is the ratio of the emission probabilities for the two types of nucleons. The abscissa, E_n or E_p is the maximum energy with which the neutron or proton can be emitted. It is equal to the nuclear excitation energy, U, minus the binding energy, B_n or B_p, of the particular nucleon.

The curves of Fig. 7 are seen to be very nearly parallel with a slowly changing slope. To make the numerical arguments simpler, let us therefore replace them by a pair of parallel straight lines whose slope, S, is the average of the slope of the curves in Fig. 7. Then the probability ordinates are

$$\ln\Gamma_n = S(E_n - E_1),$$
$$\ln\Gamma_p = S(E_p - E_2),$$

where E_1 and E_2 are the energy axis intercepts. If the excitation energy of a particular nucleus is U, then $U = E_n + B_n = E_p + B_p$. It follows that

$$\ln(\Gamma_n/\Gamma_p) = S[(B_p - B_n) + (E_2 - E_1)]. \quad (1)$$

Thus, one finds that (to the extent that one may replace the curves of Fig. 7 by straight lines), the relative emission probabilities of neutrons and protons do not depend on the excitation energy, but only on the difference between neutron and proton binding energy. From the actual curves of Fig. 7, the best average values for S and $(E_2 - E_1)$ are 0.32 Mev^{-1} and 6 Mev, respectively. It remains to express $B_p - B_n$, the difference in binding energies, in terms of the position of the nucleus with respect to the stable valley. This can be done with the help of the mass formula as it is given by Coryell.[20] If local fluctuations such as odd-even effects are overlooked, then

$$M(A,Z) = M(A,Z_A) + \frac{B_A}{2}(Z - Z_A)^2.$$

Here Z_A is the value of the atomic number at the bottom of the stable valley for the mass number A. With the help of this formula, $(B_p - B_n)$ may be written $(M_p - M_n) - B_A[x - \frac{1}{2} + (\partial Z_A/\partial A)]$, where $(M_p - M_n)$ is the proton-neutron mass difference and x is the distance, $(Z - Z_A)$, of the excited nuclide from the stable valley. For the region of nuclear masses around $A = 70$, we find[20] that $B_A = 2.6$ Mev and $(\partial Z_A/\partial A) = 0.4$. Substituting for $(B_p - B_n)$ in (1),

$$\ln(\Gamma_n/\Gamma_p) = 1.60 - 0.83x. \quad (2)$$

From a graph of this equation (Fig. 8), one can determine average neutron and proton evaporation probabilities for any excited middle weight nuclide. These probabilities depend only on the distance of the nuclide from the stable valley. It can be seen that for nuclides lying along the stable valley, neutron evaporation is about five times more probable than proton evaporation. The two evaporation probabilities are equal at roughly two units of Z (measured along constant A), to the neutron-deficient side of the stable valley.

With the help of Eq. (2) or the corresponding graph, it is possible to follow the evaporation part of a spallation reaction. The average excitation energy left in a nucleus after the nucleon collision cascade part of a reaction, may be estimated[14] to be roughly 50 Mev.

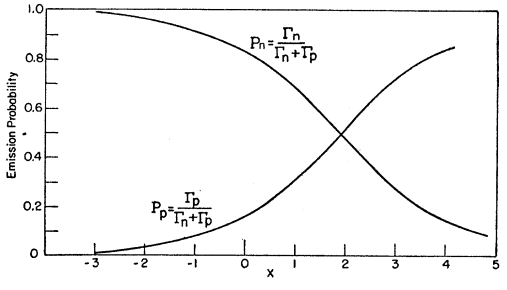

FIG. 8. The evaporation probability of neutrons and protons from medium weight nuclei (copper-arsenic mass region) as a function of x, the distance of the nucleus from the stable valley.

[20] C. D. Coryell, Ann. Rev. Nuc. Sci. 2, 305 (1953).

This is enough energy for the evaporation of four or five nucleons. According to the model of Fig. 6, the nuclides in which evaporation begins tend to lie to the proton-deficient side of the stable valley. It is possible to obtain a rough estimate of the most probable value of x at the start of the evaporation. Imagine, for example, that arsenic is the target and that ten nucleons are emitted during the nucleon-nucleon collision cascade. If equal numbers of neutrons and protons are emitted during this part of the reaction, the final nucleus is Ni^{65} for which x happens to be -1.2. Thus even for a fairly long collision cascade, the most probable final value of x is somewhere between -1 and -2. For shorter cascades, it is probably closer to -1. The distribution about this probable value is likely to be rather wide if the pre-evaporation emissions take place in a random uncorrelated way.

It turns out that the final distribution of nuclides after evaporation is not too sensitive to the distribution just before evaporation. In constructing Fig. 9, three different distributions were assumed to hold at the start of the evaporation. Final distributions were computed from these distributions by allowing 5 nucleons to evaporate one at a time. In order to construct a new distribution following an evaporation from a given distribution, one need only know the probabilities for neutron and proton emission from each nuclide in the given distribution. This information is given in Fig. 8.

In Fig. 9, the assumed starting distributions were centered at $x=-1$, 0 and 0 for the three distributions. The widths of these starting distributions were taken to be 3.7, 3.7, and 2.0, respectively. It is seen from the figure that the final distributions turn out to be very similar and therefore rather insensitive to the assumed starting distribution. The final distribution should, of course, correspond to the experimentally observed distribution and it is seen that the peaks occur at roughly half a unit of x to the neutron deficient side, just as one observes. The computed distribution widths are however about 50 percent wider than the observed widths.

Had the discrepancy been in the other direction, one could think of things that might tend to spread out the observed distribution. For example, not all nuclides are identical in their properties with respect to evaporation as we have here assumed. There are evidences for effects due to oddness or evenness of the numbers of neutrons and protons[1] in a nucleus. Any such deviations from an average behavior would tend to broaden the distribution.

Since the observed distributions are significantly narrower than the computed ones, it is worth looking hard at some of the assumptions made in the calculation.

(1) The length of the evaporation chain.—Distributions were computed for the evaporation of up to ten particles. Although the center of the distribution moves slowly toward $x=2$, the width doesn't change appreciably.

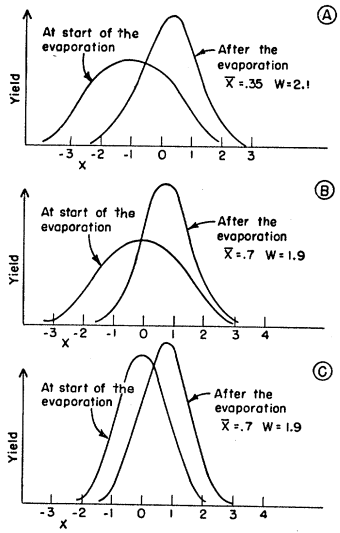

FIG. 9. The change in the distribution of nuclei, with respect to the center of the stable valley, that is brought about by the final evaporation of 5 nucleons. The locations of the centers of the final distributions and their widths are given. Three rather different starting distributions were assumed.

(2) Alpha-particle emission.—There is considerable evidence from photographic plate work[21,22] and other experiments that a fair number of α particles are emitted in spallation reactions. Their emission has been overlooked here in order to keep the calculations simple. Moreover it can be shown that α emission will not influence the width of a distribution curve unless α particles can be evaporated with high probability only from nuclides in a very limited range of x. Computations for α particles of the same sort as those leading to Fig. 8 indicate that an α particle has about a five percent chance of being evaporated at any stage of the evaporation and that this probability is hardly at all dependent on x. The only effect of α evaporation on the final distribution is to shift the peak slightly to the proton-deficient side. It does not change the width.

(3) Variation of level density with excitation energy.—The parameter S in Eq. (1) has to do with the way the nuclear level density depends on energy. In order to tighten up distribution curves, the slope, S, would have to have a larger value than the particular average value that has been assumed. It is seen that S actually increases toward the end of an evaporation (Fig. 8). Yet, it doesn't appear, on the basis of some trial calculations, that the final tightening up of yield surface due to this increase in S is sufficient to account for the narrow observed surfaces.

The calculations of this section indicate that the observed features of yield surfaces can be semiquantitatively accounted for by a model in which the last

[21] R. W. Deutsch, Phys. Rev. **90**, 499 (1953); **92**, 515 (1953).
[22] N. Page, Proc. Phys. Soc. (London) **463**, 250 (1950).

several nucleons are evaporated. The numerical discrepancies will perhaps be removed when more detailed information is available about nuclear level densities.

It should be emphasized at this point that the foregoing calculations apply only to targets of medium atomic weight. It is straightforward to carry out similar calculations for heavier targets. The most striking result of such calculations is the shift of the yield surface ridge to the neutron deficient side of the stable valley. For very heavy targets the ridge swings around until it is almost parallel to the N-axis of the isotope chart (Fig. 4). This shift is due in part to the suppression of charged particle evaporation because of the Coulomb barrier. This Coulomb effect is enhanced because the sides of the valley of the nuclear energy surface are less steep for heavy nuclei. The nuclear energy surface is therefore less able, than it is for lighter nuclei, to supply the restoring forces needed to keep a chain of evaporations confined to the neighborhood of the stable valley. Experimental results with heavy targets agree with these general conclusions. For example, Sugarman[23] found that the reaction $(\gamma,8n)$ is twice as probable as $(\gamma,p7n)$ in bismuth with 86-Mev bremsstrahlung.

6. PHOTONUCLEAR YIELDS FOR REACTIONS IN WHICH ONLY A FEW PARTICLES ARE EMITTED

The photonuclear yield data for reactions in which ΔZ is less than two do not fit the general patterns discussed in the preceding sections. It is not to be expected that such yields would fit, since yield distributions, where only a few particles are emitted, could hardly be sufficiently influenced by the nuclear energy surface. For these reactions, in which $\Delta Z \leqslant 1$, the observed yields can in most cases be assigned without ambiguity to specific isotopes in the target. They have been renormalized to a g/cm^2 of target isotope and are plotted as a function of the number of neutrons emitted. The data for reactions in which one proton (Fig. 10) and no protons (Fig. 11) are emitted are plotted separately. The dashed curve in each case is meant to represent a sort of back-extrapolation of the yield surface of the earlier sections to the region near the target. Some of the points plotted represent data obtained by other workers.[24,25]

It is seen that the yields in which two or more neutrons are emitted agree tolerably well with what one might expect on the basis of the extrapolated yield surface. But the yields for (γ,n), (γ,p), and (γ,pn) reactions are all much greater than one would expect from yield surface considerations. This fact is certainly due to the abnormally large absorption cross section for photons of about 20 Mev (the giant resonance). Indeed it can be argued that no more than 10 percent of the (γ,n) yield is due to photons in the bremsstrahlung spectrum with energies in excess of the resonance energy. From Sagane's work,[26] the ratio of the yield of the $(\gamma,2n)$ reaction to that of the (γ,n) reaction is about 0.1 for resonance photons. From the

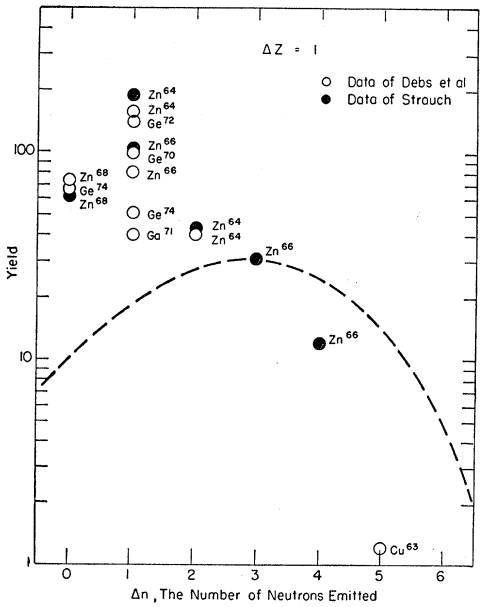

FIG. 10. A plot of the yield data for $\Delta Z=1$. The (γ,p) and (γ,pn) yields are seen to be larger than one would expect on the basis of the yield surface of Fig. 2.

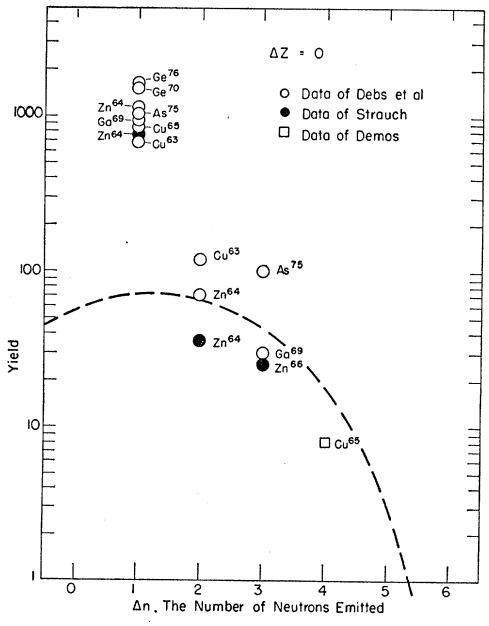

FIG. 11. A plot of the yield data for $\Delta Z=0$. The (γ,n) yields are larger than one would expect on the basis of the yield surface of Fig. 2.

[23] N. Sugarman and R. Peters, Phys. Rev. **81**, 951 (1951).

[24] K. Strauch, Phys. Rev. **81**, 973 (1951).
[25] P. T. Demos (unpublished).
[26] R. Sagane, Phys. Rev. **83**, 174 (1951).

TABLE II. Relative yields of separated elements in an irradiation of copper.

Element	ΔZ	Yield
Copper	0	900
Nickel	1	470
Cobalt	2	60
Iron	3	26
Manganese	4	11
Chromium	5	5
Vanadium and lighter elements	6	4
		Total 1476

present work, the similar ratio for 320 bremsstrahlung is less than 0.2. If one makes the reasonable assumption that the $(\gamma,2n)$ yield for post-resonance photons exceeds the (γ,n) yield for those photons, it follows that the (γ,n) yield for these photons is less than 10 percent of the resonance yield. Terwilliger[27] has been able to reduce this limit even lower.

Another noteworthy feature of the data in Figs. 10 and 11 is the spread of observed yields for (γ,n) and (γ,pn) reactions. In view of the dipole sum rule,[28] the integrated absorption cross section for resonance photons is presumably very nearly the same for all of the targets bombarded. Although part of the scatter in the data here is certainly due to experimental error, the major part is presumably due to varying degrees of competition with non-observed reactions. For example, the fact that the (γ,n) yield of Cu^{63} is 30 percent less than that of Cu^{65} has very likely to do with the fact that Cu^{63} has a lower binding energy for protons (compared to the neutron binding energy). The sum of the (γ,p) and (γ,n) yields from Cu^{63} may be very nearly equal to that from Cu^{65}. It is difficult to make very significant comparisons of observed (γ,n) yields with theoretical expectations, since neither the data nor the quantitative aspects of evaporation theory would, at present, warrant precise numerical comparison. This is especially true if one assumes that even in the resonance region, a fair fraction of the emitted neutrons and protons are directly ejected[29,30] rather than evaporated.

7. CROSS SECTIONS FOR NUCLEAR REACTIONS WITH HIGH-ENERGY X-RAYS

It is interesting to compare the yield data of the present experiment to estimates of yields for nuclear events measured in other ways. The following discussion will be restricted to a single representative medium weight target, namely, copper.

To begin with, it is possible to estimate the total number of nuclear events produced in copper by 320-Mev bremsstrahlung. One has only to supplement the yield data actually observed in copper irradiations with estimates based on interpolations of other data. One can use the yield surface, Fig. 2, and Figs. 10 and 11. In units of the preceding paper, the yields so estimated have been listed in Table II according to the separated element. To see how the listed numbers were arrived at, consider the first number, 900 units for the yield of copper isotopes. From Table I of the preceding paper the total (γ,n) yield is 740 units. The $(\gamma,2n)$ yield was measured only for Cu^{63} but assuming a comparable yield for Cu^{65}, the estimated combined yield is 120 units. The best estimate of the $(\gamma,3n)$ yield (Fig. 11) is 30 units and the yields for the production of lighter copper isotopes are smaller yet. In round numbers, the total yield of copper nuclides in a copper irradiation is 900 units. Similarly the yields of the other elements have been obtained.

TABLE III. Measurements and estimates of photonuclear yields in copper for 320-Mev bremsstrahlung (given in units of mb/Q).

Total number of events	121[a]	107[b]	
Number of "post-resonance" events	32[a]	27[b]	20[c]
Number of events made by photons of more than 150 Mev	12[c]		
Total number of neutrons emitted	180[a]	158[b]	
Number of neutrons emitted in post-resonance reactions	94[a]	78[b]	
Number of protons emitted with energies greater than 10 Mev (non-evaporated protons)	26[c]	16[d]	
Number of mesons emitted	2.1[e]	2[c]	

[a] Present work normalized as described in Sec. 7.
[b] See reference 27.
[c] S. Kikuchi, Phys. Rev. **86**, 41 (1952).
[d] J. C. Keck, Phys. Rev. **85**, 410 (1952).
[e] See references 32, 33, and 34.

It is possible to convert the arbitrary yield numbers of Table II into something more absolute by comparing our (γ,n) yield to the accurate measurements of Katz.[31] Although his measurements extend only to 25 Mev, we have seen that only a few percent of the (γ,n) yield is due to photons of higher energy. The excitation curves of Katz together with the shape of the 320-Mev x-ray spectrum lead to an estimate of 61 mb per equivalent quantum of 320-Mev x-rays for the (γ,n) yield in copper. Thus, since the (γ,n) yield of 740 units corresponds to 61 mb/Q (a Q, or equivalent quantum, contains 320 Mev of energy), the total yield (1476 units) is roughly 121 mb/Q. This number as well as estimates of some partial yields appear in Table III. One of the more interesting partial yields is that for events produced by just the resonance photons. To obtain an estimate for this yield, it is, of course, necessary to decide which of the observed yields are due to resonance photons and which are not. Because of the absence of good excitation curve data, such decisions must be somewhat arbitrary. It was assumed that all of the yield for reactions in which $\Delta A=1$, half the yield where $\Delta A=2$, and none of the yield where $\Delta A>2$, belong to the resonance. Under these assumptions only

[27] L. W. Jones and K. M. Terwilliger, Phys. Rev. **91**, 699 (1953).
[28] J. S. Levinger and H. A. Bethe, Phys. Rev. **78**, 115 (1950); **85**, 577 (1952).
[29] E. D. Courant, Phys. Rev. **82**, 703 (1951).
[30] B. C. Diven and G. M. Almy, Phys. Rev. **80**, 407 (1950).
[31] L. Katz and A. G. W. Cameron, Can. J. Phys. **29**, 518 (1951).

32 mb/Q or roughly a quarter of the total yield is due to post-resonance photons. The reason for the predominance of resonance reactions with 320-Mev x-rays is due not only to the large size of the cross section at those energies, but also to the shape of the bremsstrahlung spectrum.

Jones and Terwilliger[27] have recently determined neutron yields from copper irradiated by 320-Mev x-rays. Neutron yields can also be computed from our data by multiplying the mb/Q for each separate yield by the corresponding neutron multiplicity and adding the results. In carrying out this sum, the emission of composite particles (α particles, deuterons) was ignored. The resulting overestimate of the total neutron emission is, however, not very serious in view of the known relatively small yield of these heavier particles, the total neutron production yield comes out to be 180 mb/Q of which 94 mb/Q or roughly half is due to post resonance photons. Both these results are quite consistent with the more direct and precise measurements of Jones and Terwilliger.

For purposes of comparison, several other types of yields have been recorded in Table III. Some of these yields are due to fairly direct measurements but some are based on interpolations of data obtained for elements other than copper. For example, one of the listed meson production yields is based on the π^+ production yield in carbon,[32] the $A^{\frac{2}{3}}$ dependence of this yield,[33] on the observed ratio of π^- to π^+ production[33] and on estimates of the π^0 production rate.[34] A final estimate based on so many components is at best rather rough, but it was thought to be useful nevertheless to record a number of different types of yields in one place. If one believes all of the numbers in the table there are some disconcerting things about some of their relative sizes. For example, it is possible to estimate the yield for the production and recapture of mesons in a nucleus from the yield of those mesons that manage to get out, if one is willing to interpret the observed $A^{\frac{2}{3}}$ dependence of the meson-production cross sections in terms of a very short mean free path for mesons in nuclear matter. But such an estimate, together with a reasonable estimate for neutron multiplicity in meson-recapture events,[35] leads to an expected neutron production rate a few times larger than what is actually observed. In view of all the uncertainties involved in the determination in some of the yields quoted, it is hard to know how seriously to regard these discrepancies.

[32] J. Steinberger and A. S. Bishop, Phys. Rev. **86**, 171 (1952).
[33] R. M. Littauer and D. Walker, Phys. Rev. **82**, 746 (1951).
[34] Panofsky, Steinberger, and Steller, Phys. Rev. **86**, 180 (1952).
[35] V. Tongiorgi and D. A. Edwards, Phys. Rev. **88**, 145 (1952).

PHYSICAL REVIEW VOLUME 97, NUMBER 5 MARCH 1, 1955

Scattering of Fast Neutrons and Protons by Atomic Nuclei*

GYO TAKEDA† AND K. M. WATSON
Department of Physics, University of Wisconsin, Madison, Wisconsin
(Received November 18, 1954)

The effects of the Pauli principle on the analysis of the scattering of fast neutrons and protons by atomic nuclei are considered. This modifies the usual multiple scattering treatment of such problems in three ways: (1) It is necessary to agree on a convention for deciding which are "scattered" and which are "nuclear" nucleons. (2) The two-body scatterings obtained from the impulse approximation must be properly antisymmetrized. (3) Exchange corrections occur because of the non-orthogonality of the plane wave states for scattered particles and the states for bound particles. The latter corrections seem to be negligible for energies sufficiently high that the multiple-scattering approach is expected to be useful anyway. The present analysis is also applicable to other types of multiple-scattering problems.

I. INTRODUCTION

IN two previous publications[1,2] the theory of the scattering of fast particles by atomic nuclei was formulated as a multiple-scattering process. In the present work we wish to extend this to the scattering of fast neutrons and protons by atomic nuclei.[3] At first sight this might appear difficult, since the concept of a single particle passing through a medium and being scattered by particles of the medium does not lend itself conveniently to a description in which all the particles are treated as indistinguishable, as demanded by the Pauli principle.[4] Nevertheless, we shall be able to conclude that under such conditions that the multiple-scattering formulation is expected to be useful anyway, the Pauli principle adds no significant complication.

* Supported by grants from the National Science Foundation and from the Wisconsin Alumni Research Foundation.
† On leave from Kobe University, Kobe, Japan.
[1] K. M. Watson, Phys. Rev. **39**, 575 (1953). This paper will henceforth be referred to as I.
[2] N. C. Francis and K. M. Watson, Phys. Rev. **92**, 291 (1953). This paper will henceforth be referred to as II.
[3] G. Takeda and K. Watson, Phys. Rev. **94**, 1087 (1954), have given an application of the conclusions in the present paper.
[4] We use the generalized Pauli principle by which neutrons and protons are two states of the *nucleon*. The wave functions describing such systems are to be antisymmetrized with respect to all nucleons.